Colloid Polym Sci (2014) 292:785–795
DOI 10.1007/s00396-013-3115-6

ORIGINAL CONTRIBUTION

Synthesis and viscoelastic characterization of sulfonated chitosan solutions

Syang-Peng Rwei · Chia-Chun Lien

Received: 11 October 2013 / Revised: 3 November 2013 / Accepted: 4 November 2013 / Published online: 28 November 2013

Abstract In this study, sulfonated chitosan (SCS) with a water-soluble property was synthesized and rheologically characterized. The Maxwell Model can accurately describe a regular chitosan (CS) solution. The G′, G″ crossover shifted toward lower frequencies as the CS concentration increased, revealing an increase of relaxation time. A frequency–concentration superposition master curve of CS solution was therefore plotted and well fitted by the experiment result. However, a modified Maxwell Model, which captures the occurrence of the quasi-plateau region of G′ in the low-frequency range, representing the initially falsely connected structure between the sulfonic acid groups and the protonated ammonium groups, was proposed for the SCS solution. The crossover of G′ and G″ was found to be independent of the SCS concentration, indicating its lower molecular weight yields a high overlap concentration, Ce. The rheological properties of SCS solutions can be affected as the following factors are increased in the order of declining effect; pH level > temperature > salt concentration.

Keywords Chitosan (CS) · Sulfonated chitosan (SCS) · Maxwell model · Relaxation time · Frequency–concentration master curve

Introduction

Chitosan (CS) is the second most abundant biopolymer in the world and is known to be environmental friendly and efficiently antibacterial material. It has been widely used as a thickening agent in wastewater treatment. Its antimicrobial and biocompatible characteristics underlie its primary use in medicine, including drug delivery and wound dressing [2, 13], and numerous international patents have claimed the applications in these medical related areas. However, chitosan is not soluble in pure water; rather, it is merely soluble in a concentrated acetic-acid solution [5, 10]. Recently, chitosan has been used extensively as the nature-born antimicrobial additive in the cosmetic industry, a daily life area [21]. The need for an acetic-acid environment limits its use in such routine duties. Chitosan must therefore be modified to increase its solubility in pure water and this problem has attracted considerable interest [9, 27].

In this investigation, chitosan was reacted with "1,3-propane sultone" to generate a novel sulfonated chitosan (SCS) which is water-soluble. Notably, even the ingredient 1,3-propane-sultone is known as a potent human carcinogen, the SCS, via complete reaction and purification, is quite safe and environment friendly. The purified SCS has a potential to become a water-born antimicrobial additive or film for applications in various fields, such as cosmetic and environmental sciences. Its rheological property plays a crucial role in material processing and thus deserves to be thoroughly investigated. A viscoelastic characterization of SCS aqueous solution at a wide range of frequencies (0.01 to 100 Hz) was performed under various conditions of concentration, pH value, ionic strength, and temperature. The frequency–concentration superposition equations of the CS and SCS solutions were then proposed herein.

Experimental method

The chitosan that was used in the experiment was purchased from VA7G Bioscience (Taipei, Taiwan) in powdered form. It had a molecular weight (Mn, number average) of about 5×10^{4} and was 90 % deacetylated (DD). Deionized water with 5 wt% of acetic acid was used to prepare a regular CS solution. The acetic acid used herein was obtained from Acros and used without further purification.

S.-P. Rwei (✉) · C.-C. Lien
Institute of Organic and Polymeric Materials, National Taipei University of Technology, #1, Sec 3, Chung-Hsiao E. Rd, Taipei, Taiwan, Republic of China
e-mail: f10714@ntut.edu.tw

Scheme 1 Synthesis procedure of sulfonated chitosans

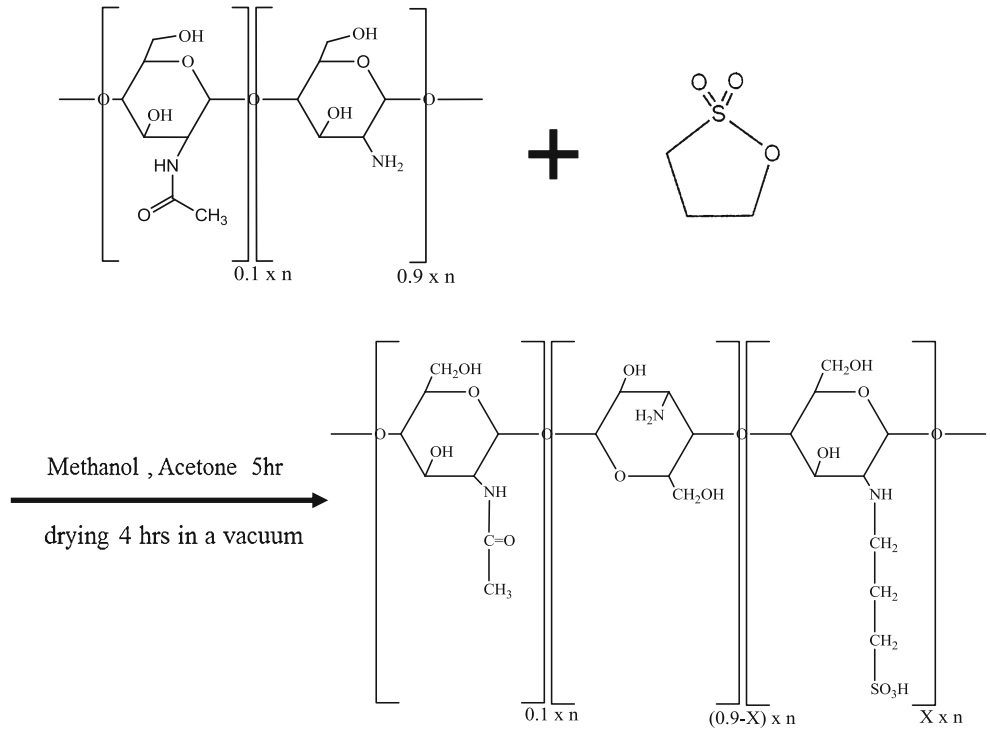

The sulfonated chitosan was prepared by modifying chitosan using 1,3-propane sultone. Five grams of chitosan was completely dissolved in 400 ml deionized water to which was added 2 wt% acetic acid. 75 ml of 1,3-propane sultone was then injected into the CS solution under nitrogen [30, 32]. The reaction proceeded at 30 °C. After a reaction time of 5 h, the solute was poured into cold acetone, causing the precipitation of product. The crude solid was washed using methanol to remove the excess 1,3-propane sultone. After drying 4 h in a vacuum oven, the SCS was obtained as a white powder at a yield of around 85 % (Scheme 1). Based on the result of element analysis shown in Table 1, the ratio of sulfonated segments is approximately 75 mole %.

Infrared spectra were obtained using a PerkinElmer Spectrum 100. ^{1}H NMR measurements were made using a Bruker Avanceat 500 MHz. D_2O was used as a solvent. GPC analyses of the copolymers were performed on a GPC/V2000 from Waters Co and AcOH (acetic acid) was used as the eluent. The steady viscosity in a Newtonian range was examined by the rheometry of Brookfield DV-III plus. Dynamic rheology was measured using a Vilastic rheometer (Vilastic Scientific Inc.) which generated an oscillatory flow using a vibratile membrane and detected the instantaneous pressure and flow rate. The samples were examined under dynamic shear of fixed but low amplitude. The shear frequency was swept over the range 10^{-2}Hz$<\omega<10^{2}$ Hz, the real part G′ and the imaginary part G″ of the shear modulus were recorded. A detailed description of the instrument and measurement can be found in the authors' earlier work [24, 25].

Results and discussion

The FT-IR spectrum of sulfonate chitosan, shown in Fig. 1, exhibits intense adsorption at 1,028, 1,148, and 1,345 cm^{-1}, corresponding to the S=O stretching vibration from the sulfonic acid group, denoted as 1. The spectrum also included strong adsorption at 1,628 and 1,517 cm^{-1}, corresponding to the C=O stretching vibration of the amide group and the C–N–C bending vibration of the SCS branch, denoted as 2. The adsorption centered at 2,922 cm^{-1} was attributed to the C–H stretching vibration of the CH_2 or CH_3 groups, denoted as 3. The FT-IR spectrum verifies the SCS synthesis. Finally, a broad peak centered at 3,311 cm^{-1} represented the combined O–H stretching vibration and N–H stretching vibration, denoted as 4.

To further confirm the success of the reaction, the ^{1}H NMR spectrum of SCS was performed. The peak position of each functional group in SCS is shown in Fig. 2. From the obtained NMR spectrum, peaks atδ=2.02–2.24 ppm(a) (−$COCH_3$ from chitin) andδ=3.71 ppm(e) were assigned for –N–CH–, and also peaks atδ=3.25 ppm(d) (−NH_2)

Table 1 The element analysis for the synthesized SCS

	N	C	Cl	S
Sulfonated Chitosan	7.08	45.04	0.28	12.00

N/S=14 (0.1*1+(0.9−X)*1+X*1)/32X=7.08/12, X=0.75

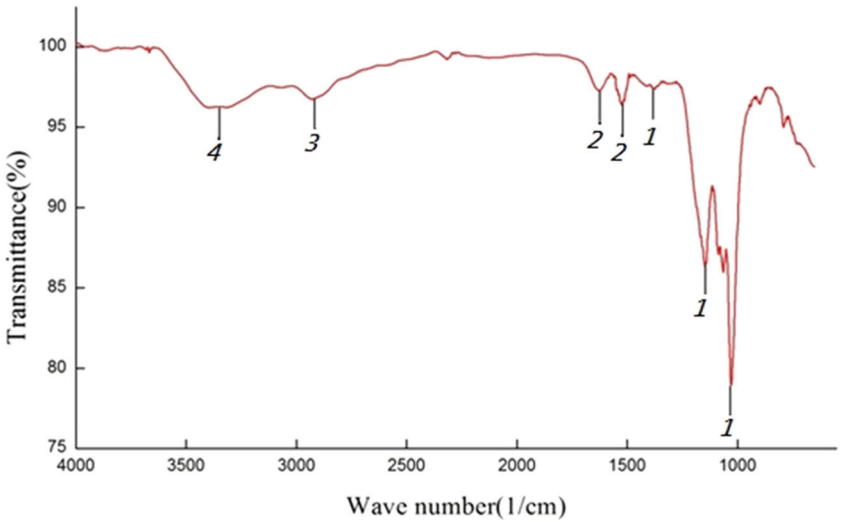

Fig. 1 The IR spectra of sulfonated chitosans

andδ=3.98 ppm(f) (−NH). Notably, peaks at 2.05 ppm (b) andδ=3.09 ppm (c) were found only for the sulfonated chitosan, which represents the $–CH_2–$ and $–SO_3H–$ groups in 1,3-propane sultone, respectively. The molecular weight and poly dispersity index (PDI) of SCS were determined by GPC using AcOH as the eluent. GPC analysis in AcOH revealed a mono-modal peak with a M_n of 13,935 and PDI (M_n/M_w) of 1.82 (Fig. 3).

Figure 4 presents the typical results of a dynamic rheological test on regular CS solutions with various concentrations. The storage (G′) and loss (G″) moduli increase with frequency. G′ typically represents elastic character while G″ represents the viscous behavior. The limiting slopes of G′ and G″ before the crossover point are 2 and 1, respectively. This result demonstrates that both structural buildup, symbolized by G′, and breakdown, symbolized by G″, increase with frequency in a low-frequency range. However, as the frequency increases, the loss modulus decays beyond the crossover point, while the storage modulus increases toward saturation. The inverse of frequency at the crossover point of G′ and G″ yields a single relaxation time of the regular CS polymer that is dissolved in aqueous solution. The single relaxation time is physically defined as the longest time required for the elastic polymer structures in the fluid to relax [1, 12, 15, 16, 23]. Interestingly, a simple Maxwell Model (Eqs. 1 and 2) [3, 18, 20, 31], comprising an elastic component (spring) in series with a viscous component (dashpot), was utilized to simulate the rheological behavior of CS solution [29], as follows.

$$G' = G_\infty(\lambda\omega)^2/\left[1+(\lambda\omega)^2\right] \tag{1}$$

$$G'' = G_\infty\lambda\omega/\left[1+(\lambda\omega)^2\right] \tag{2}$$

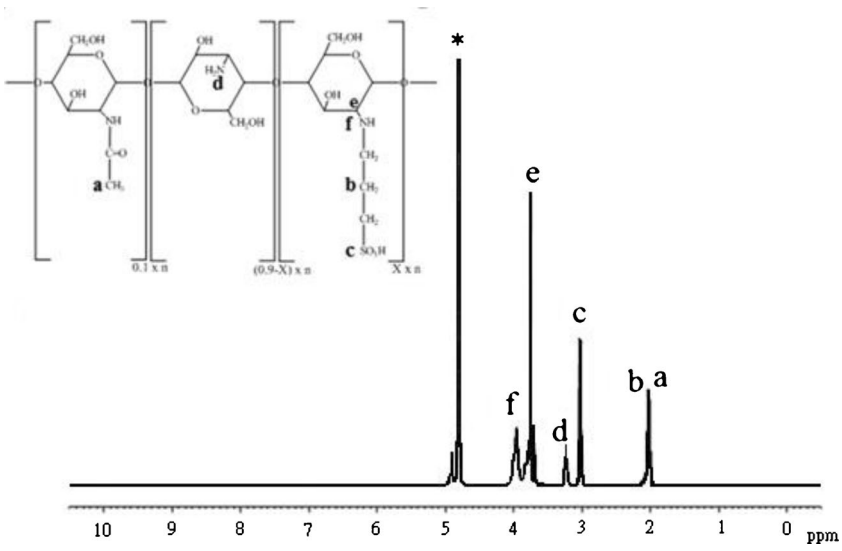

Fig. 2 The ^{1}H NMR spectra of the sulfonated chitosan

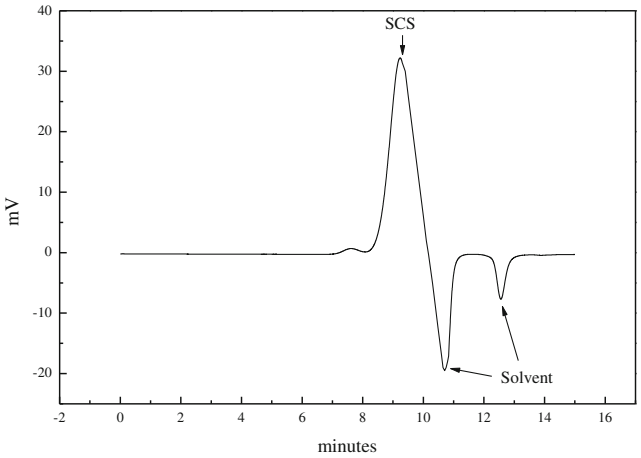

Fig. 3 The GPC plot of the sulfonated chitosan. (M_n=13,935, M_w/M_n= 1.82)

where ω denotes the applied frequency; G_∞ is a fitting parameter, is roughly equal to double of the maximum of the G″; and λ is the relaxation time, determined from the inverse of the frequency at the crossover point of G′ and G″. The simulated results (solid line) in Fig. 4 are strongly consistent with the experimental data (points) at applied frequencies from 0.01 to 20 Hz. In fact, very few materials exhibit viscoelastic spectra with a single relaxation time as in a simple Maxwell model, namely a combination of one spring and one dashpot units. A near-Maxwellian behavior is sometimes observed for self-assembled wormlike surfactant micelles or associative polymer solutions [6, 28, 35], which form transient network structures. However, viscoelastic spectra of polymer solutions measured within a limited frequency range as shown in this study can be fit to the Maxwell model well, indicating the chain conformation of CS in the acetic-acid solution is a typical random–coil type with a single relaxation time. Goodwin [8, 33] noted that the good match of a simple Maxwell Model with a single relaxation time, revealing an insignificant or even complete lack of aggregation by the hydrophobes. Hydrophobic characteristics increase aggregate size, reduce the number of aggregates, and thereby reduce energy loss during oscillation. The G″ is therefore not sensitive to the frequency and the slope of a plot of G″ as a function of frequency is therefore less than 1. Accordingly, the ratio of G′ slope/G″ slope before the crossover point is not 2, deviating from the prediction made using the Maxwell Model. Annable et al. [1] offered a similar explanation [24]. Fortunately, the strong fit of a simple Maxwell Model for a regular CS solution reveals a single relaxation time and negligible aggregation in the acetic-acid solution.

Figure 4 reveals another interesting fact: an increase in concentration results in an increase in both G′ and G″, and a clear simultaneous shifting in the crossover frequency toward lower value, indicating an increase of relaxation time with CS concentration. Increasing the CS concentration strengthens the interaction among the chains of CS molecules. If the CS concentration exceeds the overlap concentration, usually denoted as Ce (Fig. 5a), then the response of the CS molecule to the oscillation no longer depends merely on the molecule itself: it will also be influenced by the chain–chain interactions in the overlapped region, usually called “chain entanglement” among the CS molecules. In general, as the concentration of CS increased from a dilute to a concentrated state, the conformations of individual chains start to contact each other after the critical overlap concentration Ce. Further increasing the CS concentration (C>Ce), the crowd molecular chains would entangle and behave as though it were in a polymer melt. Figure 5a shows the slopes of Log (specific viscosity) against Log (concentration) at the concentration range lower and higher than Ce are 1.1 and 4.2, respectively. For

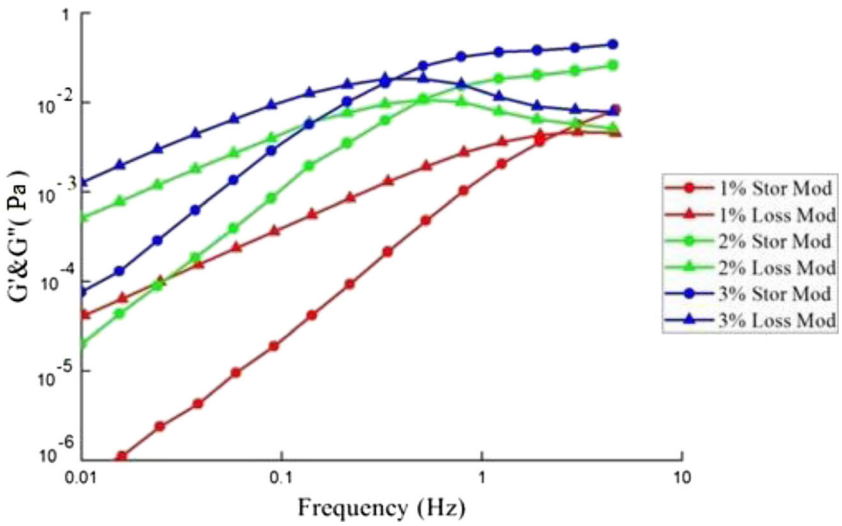

Fig. 4 Storage modulus (G′) and loss modulus (G″) for Chitosan at different concentrations (1 ~ 3 wt%)

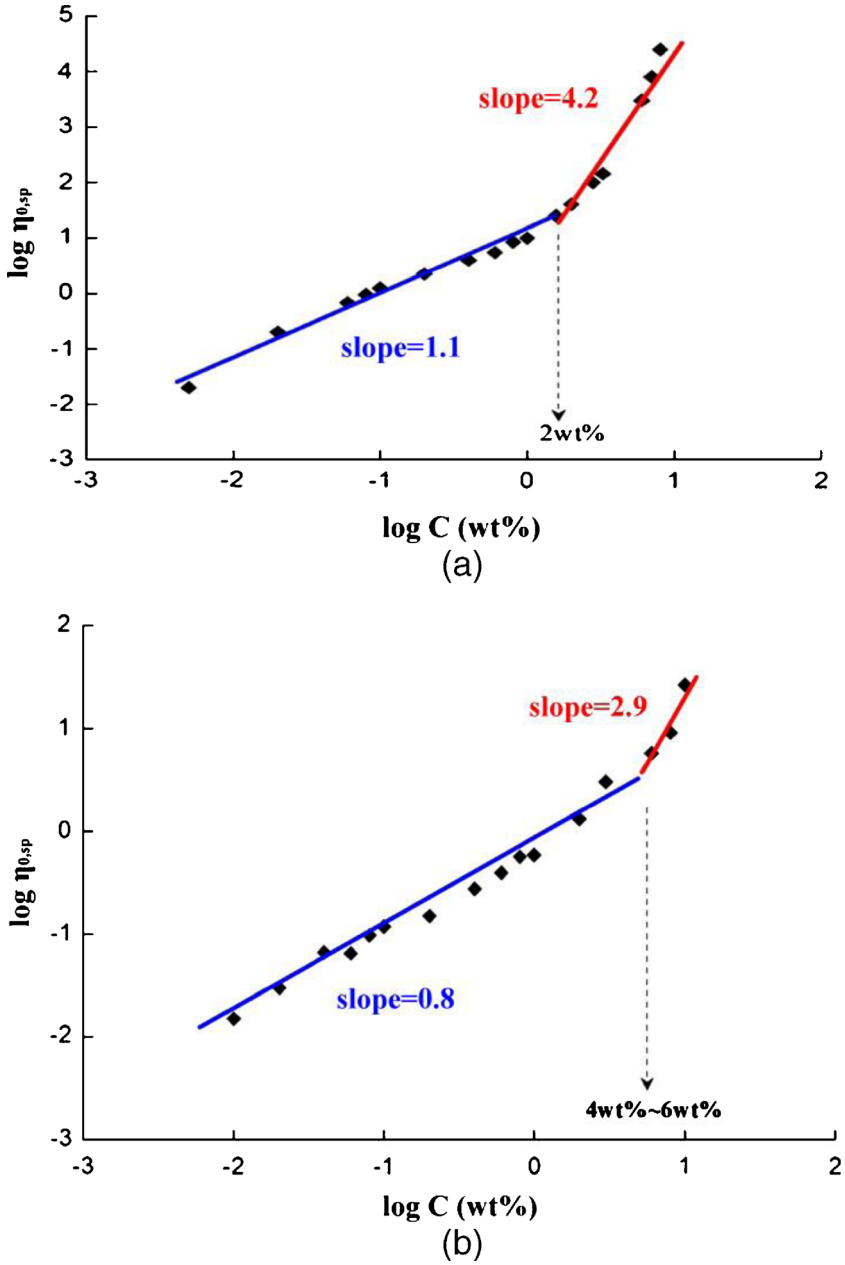

Fig. 5 The overlap concentration Ce of **a** chitosan solution and **b** sulfonated chitosan solution at 22 °C

flexible polymer solutions, the exponent of the concentration C dependence of viscosity is known to be 1 for C<Ce and 3~5 for C>Ce, respectively. The viscosity data presented herein show typical behavior of flexible polymer solutions [4, 19, 22, 26]. The relaxation time of "entangled" CS molecules is thus increased, even though all of the chain relaxation is still in a well dissolved state with no occurrence of bulky aggregation, and the G′ and G″ can be described by the simple Maxwell Model.

Figure 6 plots the master curve of Fig. 4 for the generalized relationship between moduli and frequency using a simple concentration shifting procedure that is based on Eqs. 3 and 4.

$$G'_p = G'/a_v, \quad a_v = (C/C_0), \quad a_h = \lambda\omega \tag{3}$$

$$G''_p = G''/a_v, \quad a_v = (C/C_0), \quad a_h = \lambda\omega \tag{4}$$

where G'_p and G''_p are so-called "reduced moduli." The horizontal shifting factor, a_h, and the vertical shifting factor, a_v, are defined as "$\lambda\omega$" and "the ratio of the given concentration over the referred concentration," respectively. Notably, both factors are dimensionless. This treatment is inspired by the derivation of the well-known WLF shifting equation [7, 11, 14] for the temperature shift of an amorphous polymer solid or melt. The WLF determines the temperature shift based

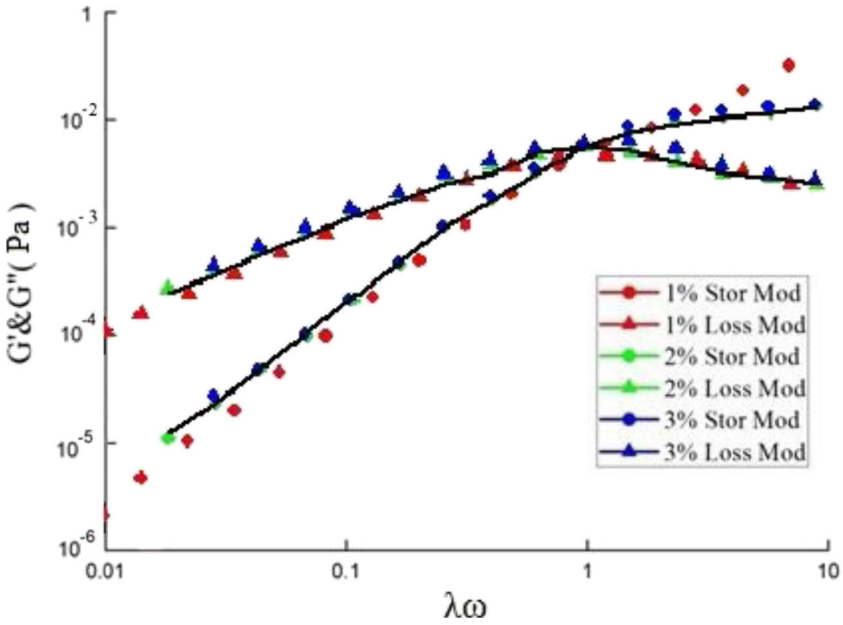

Fig. 6 Master curve of frequency–concentration superposition for chitosan solutions at different concentrations (1 ~ 3 wt%) shown in Fig. 4

on the viscosity change and an Arrhenius-type equation describing the correlation between the temperature and viscosity was used. Similarly, the viscosity change is strongly related to the difference of concentrations for various amounts of polymer dissolved in the solution. The horizontal shift, shifting along the x-axis, however, is to combine the relaxation time λ to yield a dimensionless term $\lambda\omega$. The main purpose of using the relaxation time as a weighting factor in the horizontal shift is to eliminate the chain–entanglement effect that is caused by the increase in concentration. The concentration superposition of dynamic moduli, presented in Fig. 6, exhibits perfect shifting into a single curve of G′ and G″, respectively, revealing the absence of a conformational transition or the formation of supermolecular structure under the selected operating conditions.

Figure 7 plots the dependence of G′ and G″ on frequency for the SCS solutions at various concentrations. Unlike the shift in the frequency of crossover point for a regular CS solution, shown previously, the frequency at which G′ and G″ of SCS cross each other is independent of concentration, meaning that the relaxation time is constant. The molecular weight, Mn, of regular CS is 5×10^4 g/mole, higher than that of SCS, 1.4×10^4 g/mole. The overlap concentration, Ce [17, 34] therefore exceeds that of the former (Fig. 5a) because Ce decreases with the molecular weight. An oscillation test at high frequency (>1 Hz) is conducted on a polymer solution at a concentration of less than Ce, then the chain–chain association that results from the chain entanglements of the dissolved molecules is very weak and can be neglected. A fixed relaxation time that is independent of the concentration for

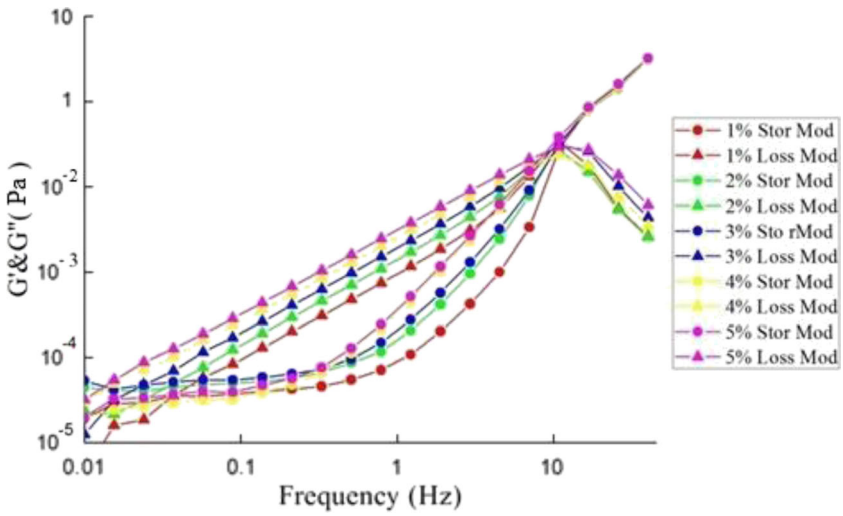

Fig. 7 Storage modulus (G′) and loss modulus (G″) for water–soluble Chitosan at different concentrations by weight (1 ~ 5 wt%). at 22 °C

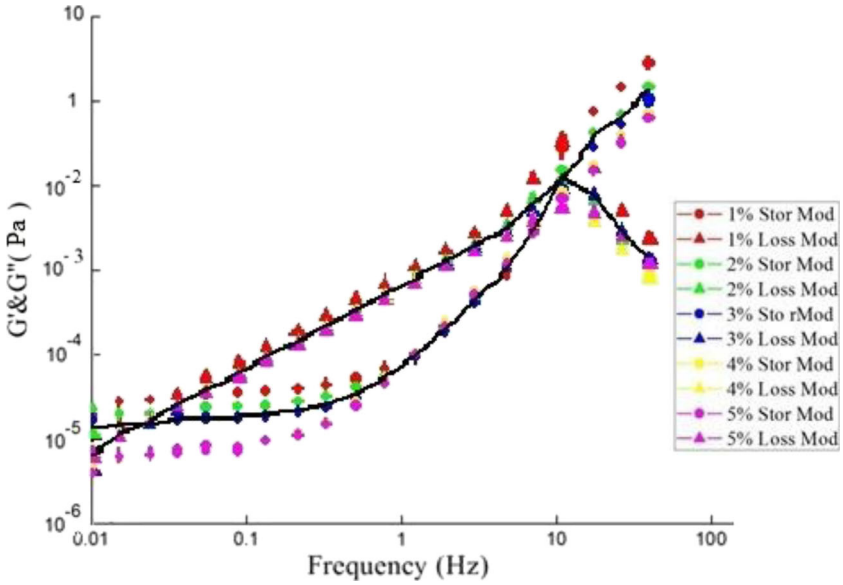

Fig. 8 Master curve of frequency–concentration superposition for SCS solutions at different concentrations (1 ~ 5 wt%) shown in Fig.7

SCS aqueous solution is thus obtained. Accordingly, the shift along the x-axis, as mentioned previously, is not required. Figure 8 plots the master curve of Fig. 7 after the shifting of the y-axis according to Eqs. 3 and 4. The curve fitting is not as close as for the CS solution because of the formation of a quasi-gel structure at low frequencies. This phenomenon will be discussed next.

Figure 9 shows a unique rheological characteristic of the SCS solution: the G″ of the Maxwell model matches perfectly the experimental data but the G′ differs substantially. A quasi-plateau region of G′ was observed at frequencies from 0.01 to 1 Hz, indicating that more energy is stored in the SCS chains than in the CS chains at a low–frequency oscillation. The sulfonic acid that is dissolved in the aqueous solution becomes a negatively charged group, whereas its ligand, positively charged acidic hydrogen, can easily attach to the amine group, NH_2, of the SCS backbone, and forming an ammonium cation, NH_3^+. The attraction between the sulfonic acid and the ammonium cation is sufficiently strong to form a weak structure under static or weakly dynamic conditions. Some of the oscillation energy can therefore be stored by the intermolecular structure and an attempt can be made subsequently to recover the work done. However, as the frequency increases, the intermolecular attraction is destroyed. Meanwhile, the Maxwell model begins to be pertinent, as it is based on a flexible chain conformation without any interaction among molecules. The quasi-plateau region at low frequency can be identified as a falsely connected state, which is similar to the formation of yield stress of a

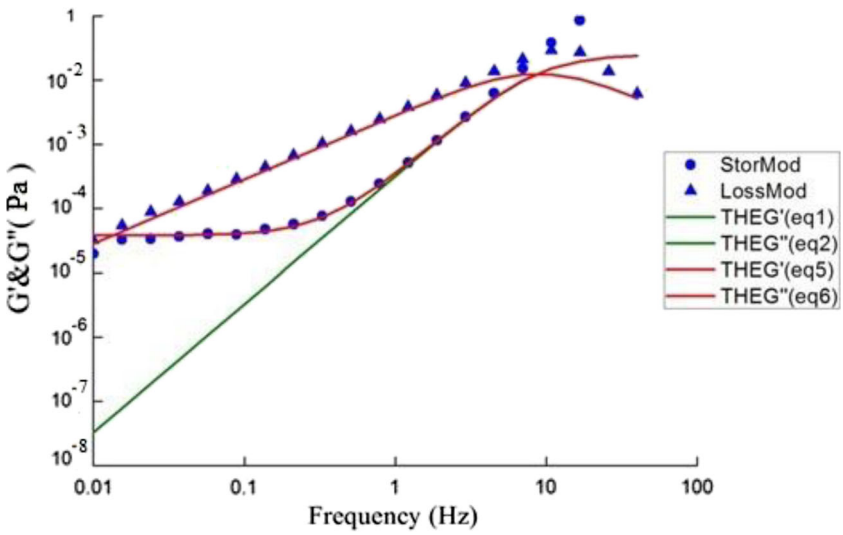

Fig. 9 Storage modulus (G′) and loss modulus (G″) for 5 % SCS solutions at 22 °C

Table 2 The rheological properties of CS and SCS solutions determined from Figs. 4 and 6

	Conc. (wt%)	ω_c (Hz)	λ (s)	G_∞ (Pa)
CS Solution	1	4.5	0.22	0.30
	2	0.51	1.96	0.32
	3	0.33	3.03	0.45
SCS Solution	1	10.80	0.093	0.30
	2	10.80	0.093	0.33
	3	10.80	0.093	0.35
	4	10.80	0.093	0.38
	5	10.80	0.093	0.38

Bingham fluid. Once the yield stress is overcome, the flow behavior of Bingham fluid is back to a normal Newtonian fluid. An extra term obtained by data fitting, G_∞ $[5.974\times10^{-4}/(\lambda\omega)^{0.1}]$, which represents the yield energy stored by the falsely connected structure and is substantial at low frequencies, is therefore added to Eq. 1 to obtain Eq. 5. The solid line in Fig. 9 is excellently fitted by Eq. 5 with a λ of 0.1349 s, validating the above hypothesis. Notably, this extra term diminishes very sharply once the frequency goes higher than 1 Hz, indicating the weakly structured state has been completely broken down into a regular viscoelastic state. The nonlinear relationship between G″ and $\lambda\omega$ shown in Eq. 6, however, is similar to Eq. 2 expressed previously. The rheological parameters, G′, G″, ω_c, and λ, which were determined by the experimental results (Figs. 4 and 7), were utilized for simulation based on Eqs. 1, 2, 5, and 6 to obtain the fitting parameter G_∞. All the experimental and fitting parameters were tabulated in Table 2.

$$G' = G_\infty(\lambda\omega)^2/\left[1+(\lambda\omega)^2\right] + G_\infty\left[5.974\times10^{-4}/(\lambda\omega)^{0.1}\right] \quad (5)$$

$$G'' = G_\infty\lambda\omega/\left[1+(\lambda\omega)^2\right] \quad (6)$$

Figure 10 plots the frequency-dependence of G' and G″ for 5 wt% SCS solutions with environment from a low pH of 2 to a moderate pH of 7, obtained by adding sodium hydroxyl. Figure 10 presents the slope of G″ decreased with increasing pH, revealing neither the simple nor the modified Maxwell model can be followed. The quasi-plateau region of G′ at low frequencies diminishes with increasing pH. An increase in pH inhibits the formation of the ammonium cation, NH_3^+. The attraction between the sulfonic acid and the ammonium cation under static or weakly dynamic conditions is therefore suppressed. Moreover, the less formation of the ammonium cation, NH_3^+, makes the water to be a poor solvent to dissolve SCS. In general, CS does not dissolve in pure water but dissolve in acetic-acid solution because that the protonation of ammonium group enhances its water solubility. Similarly, 5 wt% of SCS can well dissolve in 95 wt% of pure water due to the self-induction of ammonium protonation by the sulfonated groups of SCS, resulting in a pH value close to 2. The increase of pH in the SCS aqueous solution would suppress the protonation effect and make the water become a poor solvent as

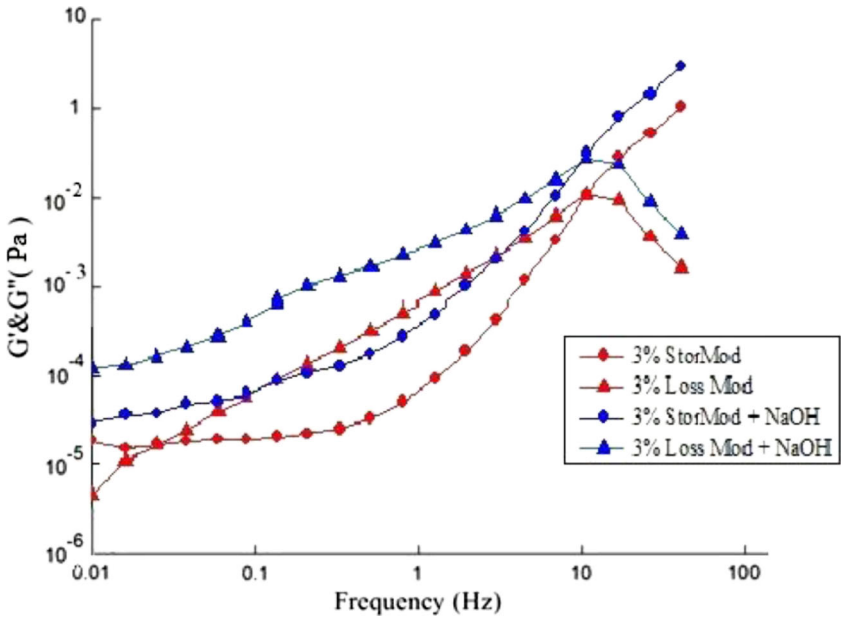

Fig. 10 Storage modulus (G′) and loss modulus (G″) for SCS solutions with addition of NaOH at 22 °C

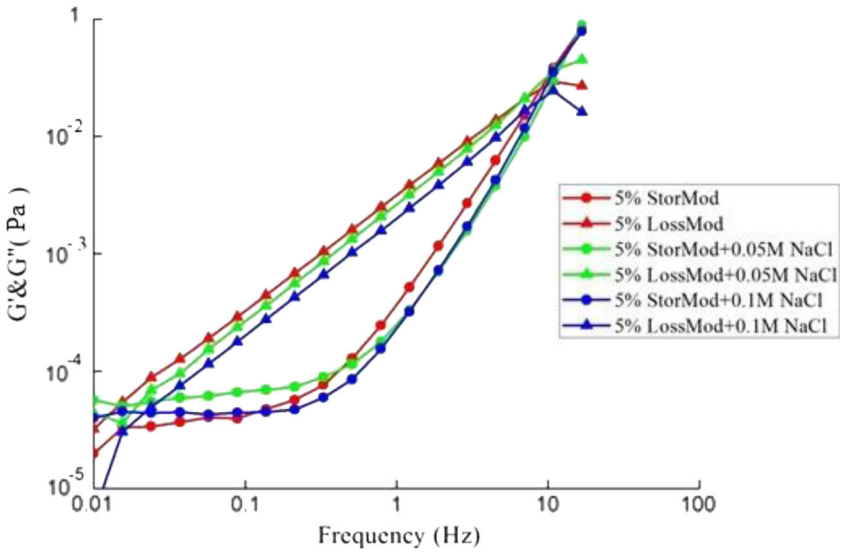

Fig. 11 Storage modulus (G′) and loss modulus (G″) for SCS solutions at 22 °C and pH of 2 but different NaCl concentrations

it does to CS. The Gaussian conformation of the random coil for SCS solution at pH of 2 under high frequency might change to a shrunken coil at pH of 7 with the slope of G′ much less than 2 as shown in Fig. 10.

Figure 11 shows the effect of adding various concentrations of sodium chloride (NaCl) to the 5 wt% SCS solution at the pH of 2. The deviation thus caused is insignificant, unlike that caused by varying pH. Since pH affects the degree of protonation of ammonium groups of SCS molecules, the effect of salt concentration on the interaction between the sulfonic acid groups and the ammonium groups could be dependent mainly on pH. As long as the pH is kept in 2, the salt effect is negligible. This result implies that the existence of Na^+ will not reduce the protonation of ammonium at low pH. It hence will not influence the random coil structure of the SCS in aqueous solution. Briefly, the conformation of the SCS did not shrink or swell with the addition of various amounts of NaCl at a low pH environment, indicating that the Na^+ or Cl^- ions do not inhibit the interaction between the sulfonic acid group and the protonated ammonium group.

The variation in temperature from 22 to 50 °C in Fig. 12 had an insignificant effect on G″, revealing that the dynamic viscosity of the SCS solution, typically denoted G''/ω, was insensitive to the temperature change. In contrast, the quasi-plateau region of G′ at low frequency became more pronounced as temperature increased. When the temperature increased, the interaction—typically hydrogen bonding between water molecules and SCS—weakened and some of the water molecules were expelled by the SCS network. The attraction between the sulfonic acid and the ammonium cation increased due to the loss of the intermediate material, the water molecules. The falsely connected state as mentioned above was thus enhanced. The results indicate that the SCS solution might have a LCST (lower critical solution temperature) behavior in a high concentration range (≫5 wt%). It is worthwhile to investigate this topic in the future.

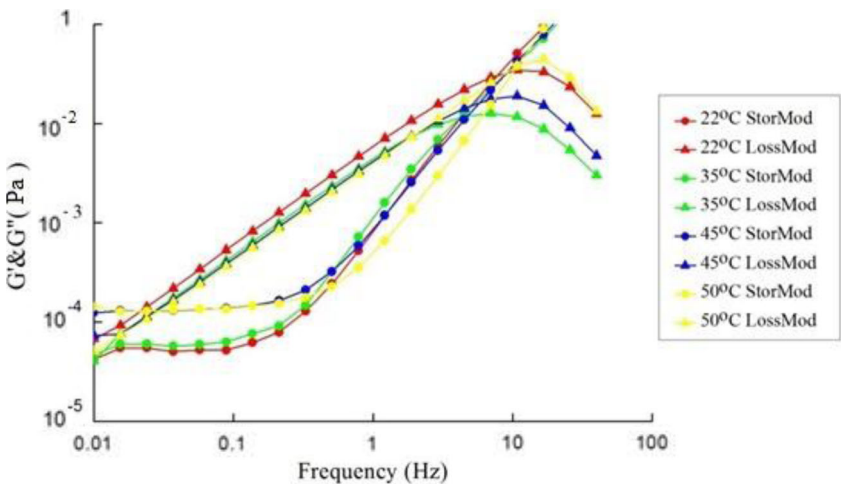

Fig. 12 Storage modulus (G′) and loss modulus (G″) for SCS solutions (5 wt%) at different temperature (22 ~ 50 °C)

Conclusions

In this study, sulfonated chitosan with a water-soluble property was successfully synthesized and rheologically characterized. The FT-IR spectrum and ^{1}H NMR analysis verify the success of SCS copolymer. A simple Maxwell Model accurately describes a regular chitosan solution. The G′ and G″ crossover shifted toward lower frequencies as the CS concentration increased, indicating an increase of relaxation time. A frequency–concentration superposition master curve was therefore plotted. However, a modified Maxwell Model, which captures the occurrence of the quasi-plateau region of G′ in the low-frequency range, representing the initially falsely connected structure between the sulfonic acid groups and the protonated ammonium groups, was proposed for the SCS solution. The crossover of G′ and G″ was found to be independent of the SCS concentration, revealing its lower molecular weight yields a high overlap concentration, Ce. The Na^{+} or Cl^{-} ions do not inhibit the interaction between the sulfonic acid group and the ammonium group, whereas the pH reduces the interaction significantly. The results presented herein demonstrate that G′ and G″ of SCS solution are affected as the following factors are increased, in order of declining impact: pH level>temperature>salt concentration.

Acknowledgment The authors would like to thank the National Science Council of the Republic of China, Taiwan, for financially supporting this research under Contract No. NSC_98-2221-E-027-004-MY3.

References

1. Annable T, Buscall R, Ettelaie R (1996) Network formation and its consequences for the physical behaviour of associating polymers in solution. Colloids Surf A Physicochem Eng Asp 112(2–3):97–116
2. Ávila A, Bierbrauer K, Pucci G, López-González M, Strumia M (2012) Study of optimization of the synthesis and properties of biocomposite films based on grafted chitosan. J Food Eng 109(4): 752–761
3. Baig C, Mavrantzas VG, Öttinger HC (2011) On Maxwell's relations of thermodynamics for polymeric liquids away from equilibrium. Macromolecules 44(3):640–646
4. Calero N, Muñoz J, Ramírez P, Guerrero A (2010) Flow behaviour, linear viscoelasticity and surface properties of chitosan aqueous solutions. Food Hydrocoll 24(6–7):659–666
5. Cho J, Heuzey M-C, Bégin A, Carreau PJ (2006) Viscoelastic properties of chitosan solutions: effect of concentration and ionic strength. J Food Eng 74(4):500–515
6. Engelskirchen S, Acharya DP, Garcia-Roman M, Kunieda H (2006) Effect of C12EOn mixed surfactant systems on the formation of viscoelastic worm-like micellar solutions in sucrose alkanoate- and CTAB-water systems. Colloids Surf A Physicochem Eng Asp 279(1–3):113–120
7. Gan W, Xiong W, Yu Y, Li S (2009) Effects of the molecular weight of poly(ether imide) on the viscoelastic phase separation of poly(ether imide)/epoxy blends. J Appl Polym Sci 114(5):3158–3167
8. Goodwin JW, Hughes RW, Lam CK, Miles JA, Warren BCH (1989) The rheological properties of a hydrophobically modified cellulose. In: Glass JE (ed) Polymers in Aqueous Media, vol 223. American Chemical Society, Washington, DC, pp 365–378
9. Hamdine M, Heuzey M-C, Bégin A (2006) Viscoelastic properties of phosphoric and oxalic acid-based chitosan hydrogels. Rheol Acta 45(5):659–675
10. Jocic D, Julia MR, Erra P (1996) The time dependence of chitosan/nonionic surfactant solution viscosity. Colloid Polym Sci 274(3): 375–383
11. Kohga M (2011) Viscoelastic behavior of hydroxyl terminated polybutadiene containing glycerin. J Appl Polym Sci 122(1):706–713
12. Larson RG (1988) Constitutive Equations for Polymer Melts and Solutions, 1st edn. Butterworths, Boston
13. Lee SY, Kim JH, Kuon IC, Jeong SY (2000) Self-aggregates of deoxycholic acid-modified chitosan as a novel carrier of adriamycin. Colloid Polym Sci 278:1216–1219
14. Lelli G, Terenzi A, Kenny JM, Torre L (2009) Modelling of the chemo-rheological behavior of thermosetting polymer nanocomposites. Polym Compos 30(1):1–12
15. Likhtman AE, McLeish TCB (2002) Quantitative theory for linear dynamics of linear entangled polymers. Macromolecules 35(16): 6332–6343
16. Likthman AE, Marques GM (2006) First-passage problem for the Rouse polymer chain: an exact solution. Europhys Lett 75(6):971–977
17. Mahaut F, Chateau X, Coussot P, Ovarlez G (2008) Yield stress and elastic modulus of suspensions of noncolloidal particles in yield stress fluids. J Rheol 52(1):287–313
18. Molchanov VS, Philippova OE (2009) Effects of concentration and temperature on viscoelastic properties of aqueous potassium oleate solutions. Colloid J 71(2):239–245
19. Morris ER, Cutler AN, Ross-Murphy SB, Rees DA, Price J (1981) Concentration and shear rate dependence of viscosity in random coil polysaccharide solutions. Carbohydr Polym 1(1):5–21
20. Papoulia KD, Panoskaltsis VP, Kurup NV, Korovajchuk I (2010) Rheological representation of fractional order viscoelastic material models. Rheol Acta 49(4):381–400
21. Peak CW, Wilker JJ, Schmidt G (2013) A review on tough and sticky hydrogels. Colloid Polym Sci 291:2031–2047
22. Pereira MC, Wyn-Jones E, Morris ER, Ross-Murphy SB (1982) Characterisation of interchain association in polysaccharide solutions by ultrasonic relaxation and velocity. Carbohydr Polym 2(2):103–113
23. Pottier N (2011) Relaxation time distributions for an anomalously diffusing particle. Phys A: Stat Mech Appl 390(16): 2863–2879
24. Rwei SP, Lee HY, Yoo SD, Wang LY, Lin JG (2005) Magnetorheological characteristics of aqueous suspensions that contain Fe_3O_4 nanoparticles. Colloid Polym Sci 283(11): 1253–1258
25. Rwei SP, Chen SW, Mao CF, Fang HW (2008) Viscoelasticity and wearability of hyaluronate solutions. Biochem Eng J 40(2):211–217
26. Seale R, Morris ER, Rees DA (1982) Interactions of alginates with univalent cations. Carbohydr Res 110(1):101–112
27. Seetapan N, Mai-ngam K, Plucktaveesak N, Sirivat A (2006) Linear viscoelasticity of thermoassociative chitosan-g-poly(*N*-isopropylacrylamide) copolymer. Rheol Acta 45(6):1011–1018
28. Simi CK, Abraham TE (2010) Transparent xyloglucan-chitosan complex hydrogels for different applications. Food Hydrocoll 24(1):72–80
29. Steffe JF (1996) Rheological Methods in Food Process Engineering, 2nd edn. Freeman Press, East Lansing (Chapter 5)
30. Türk H, Haag R, Alban S (2004) Dendritic polyglycerol sulfates as new heparin analogues and potent inhibitors of the complement system. Bioconjug Chem 15(1):162–167

31. van de Manakker F, Vermonden T, el Morabit N, van Nostrum CF, Hennink WE (2008) Rheological behavior of self-assembling PEG-β-cyclodextrin/PEG-cholesterol hydrogels. Langmuir 24(21): 12559–12567
32. Van Vlierberghe S, Dubruel P, Schacht E (2011) Biopolymer-based hydrogels as scaffolds for tissue engineering applications: a review. Biomacromolecules 12(5):1387–1408
33. Vermonden T, van Steenbergen MJ, Besseling NAM, Marcelis ATM, Hennink WE, Sudhölter EJR, Cohen Stuart MA (2004) Linear rheology of water-soluble reversible neodymium(III) coordination polymers. J Am Chem Soc 126(48): 15802–15808
34. Wang Q, Yang Y, Chen X, Shao Z (2012) Investigation of rheological properties and conformation of silk fibroin in the solution of AmimCl. Biomacromolecules 13(6):1875–1881
35. Yesilata B, Clasen C, McKinley GH (2006) Nonlinear shear and extensional flow dynamics of wormlike surfactant solutions. J Non-Newtonian Fluid Mech 133(2–3):73–90